

Confined Vibe Optimization: Closed-Loop Text-to-Appearance Inverse Rendering with Vision-Language Feedback

Chi-Chang Lee

University of Maryland, College Park

changlee@umd.edu

Wenxuan Wu

University of Maryland, College Park

wenxuan6@terpmail.umd.edu

Abstract

We study an unpaired text-to-appearance inverse rendering problem: given only a text instruction, we optimize a differentiable renderer's continuous control parameters to synthesize an image that matches the requested look. Direct CLIP-driven optimization is often unstable and under-constrained, frequently yielding attribute entanglement or degenerate solutions. We propose a closed-loop method that uses a vision-language model to (i) parse the current rendering into foreground and background objects with attributes, producing swap-safe prompt augmentations, and (ii) generate a parameter-wise optimization plan that selects a small set of parameters to update and restricts their feasible ranges. We then perform differentiable optimization under this plan using a region-aware CLIP objective and stability safeguards. Experiments show improved overall prompt adherence and object visibility compared to a naive CLIP-only baseline, and ablations indicate that our method supports controllable refinement under prompt extension while remaining robust when instructions are semantically underspecified. GitHub: <https://github.com/ChangLee0903/Vibe-Rendering>

1. Introduction

Inverse rendering aims to recover physically meaningful scene parameters, commonly geometry, material reflectance, and illumination, from one or more images, enabling relighting, retexturing, and physically grounded scene understanding. Despite decades of progress, inverse rendering remains fundamentally ill posed due to strong ambiguities among appearance factors, for example albedo and illumination trade offs, and the presence of global illumination effects. Classical analyses provide theoretical foundations for estimating lighting and reflectance and for characterizing these ambiguities [6, 8]. More recently, learning based approaches improve robustness by combining differentiable rendering with priors learned from

data, often trained on large scale physically based synthetic datasets where ground truth intrinsics are available [4, 9]. However, such progress typically depends on paired supervision, either explicit ground truth decompositions and scene parameters or tightly controlled capture setups, because real world imagery rarely comes with paired target renderings or accurate per scene labels for geometry, lighting, and SVBRDF, motivating methods that operate with weaker, unpaired forms of supervision [4, 9].

A growing body of work therefore explores unpaired, target free inverse rendering by replacing pixel aligned targets with high level constraints provided by multimodal foundation models. One line of research uses pretrained image text encoders as differentiable objectives, optimizing a renderable 3D representation so that differentiably rendered images match a language description in a joint embedding space, for example CLIP guided optimization of textured meshes [3]. Another line leverages pretrained text to image diffusion models as powerful natural image priors, distilling their guidance through differentiable rendering to optimize 3D parameters without paired targets, popularized by score distillation objectives and extended to higher quality mesh based pipelines [5, 7]. Subsequent work improves stability and diversity through refined distillation formulations such as variational score distillation [10]. Complementarily, instruction guided pipelines demonstrate that diffusion based image editing can be coupled with 3D optimization loops to impose textual edits consistently across views [1, 2], highlighting the promise of language as a flexible supervisory signal when paired targets are unavailable.

Existing unpaired formulations, however, are still far from delivering reliable parameter estimation in realistic inverse rendering settings. Because language or generative priors supervise images at semantic or perceptual levels, optimization can exploit shortcut solutions that satisfy the prompt while drifting away from plausible parameters, and these failure modes are exacerbated by the intrinsic ambiguities of inverse rendering [6, 8]. This challenge becomes particularly acute when the optimization variables are high dimensional or over parameterized, leading to un-

stable convergence, poor identifiability, and inconsistent results across views, which has been widely observed in diffusion guided optimization settings [7, 10]. Moreover, many prior unpaired methods optimize implicit 3D representations or free form textures, whereas practical inverse rendering pipelines often require structured, physically interpretable parameter sets with explicit bounds, sharing constraints, and trainable or frozen decisions [4]. In this work, we propose a language constrained inverse rendering framework that turns unpaired supervision into actionable and stable parameter updates by explicitly confining the optimization space. Our key idea is to introduce a constraint designer, implemented with a vision language model, that takes rendered images, a structured parameter specification, and textual feedback as input and outputs a parameter wise optimization plan, including which parameters are trainable, which are shared or locked to prevent scale ambiguities, and what tightened confidence ranges and priors should be applied. The differentiable renderer then optimizes only within this confined space under language based guidance, and the updated renderings are fed back for iterative refinement. This closed loop interaction stabilizes optimization in the absence of paired targets while preserving physically interpretable controls and preventing common degeneracies.

Contributions. This paper makes three contributions. First, we formulate unpaired inverse rendering as a closed loop optimization problem in which language and vision foundation models provide supervision in lieu of paired target images, while a differentiable renderer supplies gradients to structured scene parameters. Second, we introduce a constraint designer that produces parameter wise optimization plans, including trainable versus frozen decisions, parameter sharing to mitigate scale ambiguities, and tightened confidence ranges with optional priors, enabling stable optimization for complex parameterizations. Third, we propose an interactive refinement protocol that alternates between constrained differentiable optimization and constraint redesign, and we show that this interaction improves convergence, controllability, and robustness under purely unpaired, instruction driven supervision.

2. Related Work

Inverse rendering has been studied extensively, with early work analyzing the ambiguity between reflectance and illumination and establishing principled formulations for recovering intrinsic components [6, 8]. Learning based inverse rendering methods commonly combine differentiable rendering with learned priors and rely on synthetic supervision, particularly for indoor scenes with spatially varying lighting and SVBRDF [4, 9]. While these approaches can be accurate under paired supervision, they face a supervision gap in realistic settings where ground truth parameters

or paired target renderings are unavailable.

Recent unpaired alternatives replace pixel aligned targets with language and generative priors. CLIP guided optimization maximizes similarity between rendered images and textual descriptions in a joint embedding space, enabling text driven mesh and texture optimization without paired targets [3]. Diffusion guided approaches distill gradients from pretrained text to image diffusion models through differentiable rendering, enabling target free optimization of 3D representations, as demonstrated by score distillation objectives and mesh refinement pipelines [5, 7]. Follow up work improves stability and diversity by modifying the distillation objective, for example via variational formulations [10]. Instruction guided pipelines further demonstrate that textual edits can be applied consistently across views by coupling diffusion based editing with 3D optimization loops [1, 2]. Despite these advances, reliable parameter estimation remains challenging when the optimization space is large and structured, motivating methods that explicitly control trainable sets, parameter tying, and feasible ranges.

3. Method

3.1. Problem Setup

We optimize a differentiable renderer \mathcal{R} that maps a structured scene parameter vector θ to an RGB image:

$$\mathbf{I} = \mathcal{R}(\theta). \quad (1)$$

The parameter vector θ spans camera configuration, illumination, material like shading controls, participating media effects (fog), and post processing. Supervision is unpaired: we are given only a text instruction t describing a target appearance, without any reference image. The goal is to estimate θ such that the rendered image is semantically aligned with t under a vision language similarity metric, while maintaining numerical stability during gradient based optimization.

3.2. Differentiable Parameterization and Rendering

We design θ as a collection of continuous, differentiable variables so that gradients can flow from an image level objective back to each controllable factor. The parameterization includes camera viewpoint, light intensity and color with an ambient term, material like controls that affect diffuse and specular appearance, fog terms that modulate depth and height dependent attenuation, and post processing controls such as exposure, contrast, hue, saturation, gamma, and vignetting. To ensure stable optimization under weak supervision, each parameter is constrained to a feasible domain via projection after every update. We additionally sanitize non finite values and apply gradient norm clipping to prevent exploding updates.

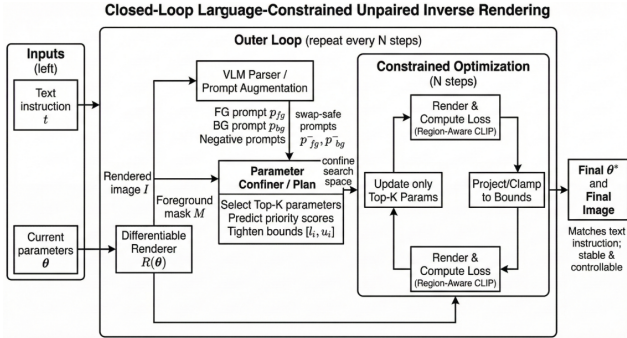


Figure 1. System Diagram.

176

3.3. Overview

177 Our approach performs unpaired inverse rendering by alternating
 178 between constrained gradient descent and language
 179 mediated constraint redesign. At each outer round, we first
 180 render the current image and extract a soft foreground mask.
 181 We then parse the current rendering together with the user
 182 instruction into an objects list with region specific attributes,
 183 and convert these structured attributes into swap safe fore-
 184 ground and background prompts plus negative prompts.
 185 Next, a confiner produces a parameter wise plan consisting
 186 of refined feasible ranges and priority scores. We select
 187 a top K subset of parameters by priority for gradient up-
 188 dates while enforcing the refined ranges for all parameters
 189 through projection. Finally, we run a fixed number of inner
 190 optimization steps using region decomposed vision lan-
 191 guage losses, followed by numerical stabilization through
 192 projection and non finite repair. The full procedure is sum-
 193 marized in Algorithm 1 and Figure 1.

194

3.4. Text Guidance via Vision Language Similarity

195 We supervise optimization using a pretrained vision lan-
 196 guage model that embeds images and texts into a shared
 197 space. Let $\mathcal{E}_I(\cdot)$ and $\mathcal{E}_T(\cdot)$ denote the image and text en-
 198 coders. For a rendered image \mathbf{I} and a prompt \mathbf{p} , we define
 199 cosine similarity

$$s(\mathbf{I}, \mathbf{p}) = \left\langle \frac{\mathcal{E}_I(\mathbf{I})}{\|\mathcal{E}_I(\mathbf{I})\|}, \frac{\mathcal{E}_T(\mathbf{p})}{\|\mathcal{E}_T(\mathbf{p})\|} \right\rangle. \quad (2)$$

201

We minimize a positive alignment loss

$$\mathcal{L}_{pos}(\mathbf{I}, \mathbf{p}) = 1 - s(\mathbf{I}, \mathbf{p}), \quad (3)$$

202

and use a hinge style negative loss to discourage forbidden
 203 concepts:

$$\mathcal{L}_{neg}(\mathbf{I}, \mathbf{p}^-) = \max(0, s(\mathbf{I}, \mathbf{p}^-) - m), \quad (4)$$

204

where m is a margin. The negative term is critical in our
 205 setting because unpaired text supervision can otherwise be
 206 satisfied through unintended attribute transfer, such as back-
 207 ground attributes leaking into the foreground or vice versa.

Algorithm 1 Region aware language constrained unpaired inverse rendering

Require: Differentiable renderer \mathcal{R} , initial parameters $\theta^{(0)}$, text instruction t , outer rounds R , inner steps T , optimization budget K .

- 1: **for** $r = 0$ to $R - 1$ **do**
- 2: Render image and mask: $(\mathbf{I}^{(r)}, M^{(r)}) \leftarrow \mathcal{R}(\theta^{(r)})$.
- 3: Parse objects and attributes: $\mathcal{O}^{(r)} \leftarrow \text{Parse}(\mathbf{I}^{(r)}, t)$.
- 4: Build prompts: $(\mathbf{p}_{fg}, \mathbf{p}_{bg}, \mathbf{p}_{fg}^-, \mathbf{p}_{bg}^-) \leftarrow \text{Compose}(\mathcal{O}^{(r)}, t)$.
- 5: Confiner plan: for each parameter θ_i , predict bounds $[l_i, u_i]$ and priority π_i using $(\mathbf{I}^{(r)}, t, \mathbf{p}_{fg}, \mathbf{p}_{bg})$.
- 6: Select update set: $\mathcal{S}_K^{(r)} \leftarrow \text{TopK}(\{\theta_i\}, \pi_i, K)$.
- 7: Apply bounds to all parameters by projection: $\theta^{(r)} \leftarrow \Pi_{[l,u]}(\theta^{(r)})$.
- 8: **for** $t = 1$ to T **do**
- 9: Render: $(\mathbf{I}, M) \leftarrow \mathcal{R}(\theta)$.
- 10: Masked images: $\mathbf{I}_{fg} \leftarrow \mathbf{I} \odot M, \mathbf{I}_{bg} \leftarrow \mathbf{I} \odot (1-M)$.
- 11: Compute loss \mathcal{L} using region positives and negatives:
- 12:
$$\mathcal{L} \leftarrow \lambda_{fg}\mathcal{L}_{pos}(\mathbf{I}_{fg}, \mathbf{p}_{fg}) + \lambda_{bg}\mathcal{L}_{pos}(\mathbf{I}_{bg}, \mathbf{p}_{bg}) + \lambda_{full}\mathcal{L}_{pos}(\mathbf{I}, t) + \lambda_{neg}(\mathcal{L}_{neg}(\mathbf{I}_{fg}, \mathbf{p}_{fg}^-) + \mathcal{L}_{neg}(\mathbf{I}_{bg}, \mathbf{p}_{bg}^-))$$
.
- 13: Gradient update only on $\mathcal{S}_K^{(r)}$: $\theta \leftarrow \theta - \eta \nabla_{\theta_{\mathcal{S}_K^{(r)}}} \mathcal{L}$.
- 14: Stabilize: clip gradient norms, project $\theta \leftarrow \Pi_{[l,u]}(\theta)$, repair non finite values.
- 15: **end for**
- 16: Set $\theta^{(r+1)} \leftarrow \theta$.
- 17: **end for**
- 18: **return** Estimated parameters $\theta^{(R)}$.

3.5. Region Aware Prompt Decomposition with Objects and Attributes

A single text instruction often entangles foreground and background attributes, and abstract style words may not directly map to optimizable parameters. To reduce ambiguity, we introduce a scene parsing module that converts the input text and the current rendered image into an explicit set of objects and their attributes.

Given the current rendering \mathbf{I} and instruction t , the parser outputs an *objects list* $\mathcal{O} = \{o_j\}$, where each object o_j is assigned to a region $r_j \in \{\text{fg, bg}\}$ and accompanied by a structured attribute dictionary \mathbf{a}_j . Attributes include color, material cues, lighting descriptors, style descriptors, mood words, and coarse shape descriptors. When the instruction contains abstract terms such as cozy, cinematic, or dreamy, the parser grounds them into visually actionable attributes conditioned on the image context, for example warm soft lighting, low contrast, gentle vignetting, or slight desatu-

210

211

212

213

214

215

216

217

218

219

220

221

222

223

224

225

226

227

228 ration. This grounding step converts vague language into
 229 constraints that can be expressed through the available pa-
 230 rameter families.
 231

From \mathcal{O} we derive region specific prompts:

$$\mathbf{p}_{fg} = \text{Prompt}(\{o_j : r_j = fg\}), \quad (5)$$

$$\mathbf{p}_{bg} = \text{Prompt}(\{o_j : r_j = bg\}), \quad (6)$$

234 together with swap prevention negative prompts \mathbf{p}_{fg}^- and
 235 \mathbf{p}_{bg}^- that explicitly forbid foreground attributes in the back-
 236 ground and background attributes in the foreground. The
 237 resulting prompts are short, region specific, and designed to
 238 minimize attribute swapping.

239 3.6. Confiner: Priority Based Parameter Selection 240 and Range Refinement

241 Even with improved prompts, many parameters remain cou-
 242 pled and can compensate for each other. Optimizing all pa-
 243 rameters simultaneously often leads to degenerate solutions.
 244 We therefore introduce a confiner module that produces a
 245 parameter wise optimization plan conditioned on the cur-
 246 rent image and the decomposed prompts.

247 For each parameter θ_i , the confiner predicts (i) a feasible
 248 range $[l_i, u_i]$ (or component wise bounds for vector parame-
 249 ters), and (ii) an integer priority score π_i indicating how im-
 250 portant it is to optimize this parameter in the current outer
 251 round. The confiner is informed by the instruction, region
 252 specific prompts \mathbf{p}_{fg} and \mathbf{p}_{bg} , negative prompts, and the
 253 current rendering, enabling it to focus on parameters most
 254 likely to explain the remaining mismatch.

255 We enforce a top K optimization budget. Let \mathcal{S}_K be the
 256 set of K parameters with the smallest priorities among those
 257 deemed relevant. Only parameters in \mathcal{S}_K receive gradients
 258 in the subsequent inner loop, while all other parameters are
 259 held fixed:

$$\mathcal{S}_K = \text{TopK}(\{\theta_i\}, \pi_i, K), \quad \nabla_{\theta_i} \mathcal{L} = 0 \text{ for } \theta_i \notin \mathcal{S}_K. \quad (7)$$

260 Separately, the confiner provided bounds are applied to all
 261 parameters through projection, which prevents drift even for
 262 frozen parameters. This separation between *range refine-
 263 ment* (global) and *gradient updates* (top K) improves iden-
 264 tifiability and stability.

266 3.7. Region Decomposed Objective and Closed 267 Loop Optimization

268 We optimize an objective that explicitly separates fore-
 269 ground and background alignment. Let M denote a soft
 270 foreground mask obtained from rendering, and define fore-
 271 ground and background composites \mathbf{I}_{fg} and \mathbf{I}_{bg} by mask-
 272 ing:
 273

$$\mathbf{I}_{fg} = \mathbf{I} \odot M, \quad \mathbf{I}_{bg} = \mathbf{I} \odot (1 - M). \quad (8)$$

274 We combine region specific positive losses, a global pos-
 275 itive loss, and negative losses:
 276

$$\mathcal{L} = \lambda_{fg} \mathcal{L}_{pos}(\mathbf{I}_{fg}, \mathbf{p}_{fg}) + \lambda_{bg} \mathcal{L}_{pos}(\mathbf{I}_{bg}, \mathbf{p}_{bg}) \quad (9)$$

$$+ \lambda_{full} \mathcal{L}_{pos}(\mathbf{I}, \mathbf{t}) + \lambda_{neg} \left(\mathcal{L}_{neg}(\mathbf{I}_{fg}, \mathbf{p}_{fg}^-) \right. \quad (277)$$

$$\left. + \mathcal{L}_{neg}(\mathbf{I}_{bg}, \mathbf{p}_{bg}^-) \right). \quad (278)$$

279 Optionally, when the instruction specifies a concrete
 280 background color, we add a weak color prior on the mean
 281 background color. We also add a boundary penalty that dis-
 282 courages the foreground mask from collapsing onto the im-
 283 age borders, which reduces trivial solutions caused by crop-
 284 ping.

285 Our overall procedure alternates between (i) parsing and
 286 prompt decomposition, (ii) confiner based plan generation
 287 with priorities and bounds, and (iii) constrained gradient de-
 288 cent on the selected top K parameters for a fixed number
 289 of inner steps. After each inner step, we project param-
 290 eters back to feasible ranges and repair numerical issues.
 291 This outer loop repeats until convergence or a fixed budget
 292 is reached, yielding a parameter estimate that matches the
 293 instruction while remaining stable under optimization.

294 4. Experiments

295 We evaluate our approach on one benchmark comparison
 296 and two ablation studies. The benchmark compares our
 297 full method against a naive CLIP-only optimization base-
 298 line to test whether structured parameter control and our
 299 guidance strategy improve text adherence and object visi-
 300 bility under the same differentiable renderer. The first ab-
 301 lation studies prompt specificity by contrasting concrete,
 302 renderer-supported attribute language with an abstract de-
 303 scription for the same object, probing robustness under se-
 304 mantically underspecified instructions. The second abla-
 305 tion studies prompt length via incremental extension, ex-
 306 amining whether adding constraints yields predictable and
 307 controllable changes in appearance rather than destabiliz-
 308 ing optimization. Together, these configurations are de-
 309 signed to isolate three practical questions in unpaired text-
 310 to-appearance inverse rendering: whether our method out-
 311 performs a direct CLIP objective, whether it remains stable
 312 under ambiguous semantics, and whether it supports con-
 313 trollable refinement as more information is provided.

314 4.1. Experimental Setup

315 We optimize differentiable renderer parameters from a fixed
 316 initialization for each object. The parameter set includes
 317 camera pose and field-of-view, point and ambient illumina-
 318 tion, material-like controls (diffuse tint, specular strength
 319 and color, roughness, shininess), fog parameters, and post-
 320 processing parameters (exposure, contrast, saturation, hue
 321 shift, gamma, vignette). All parameters are updated via

322 gradient-based optimization through the renderer at $512 \times$
 323 512 resolution for a fixed iteration budget.

- 324
- **Baseline (CLIP-only).** The baseline performs end-to-end optimization using a single global CLIP alignment
 325 loss between the full rendered image and the raw user
 326 prompt. It does not use region decomposition, negative
 327 constraints, or any external model guidance.
 - **Ours.** Our method augments CLIP guidance with struc-
 328 tured text supervision that separates foreground and back-
 329 ground intent and introduces constraints that discourage
 330 attribute leakage across regions. In addition, we use a
 331 VLM-guided step to restrict the search to a small subset
 332 of parameters at each stage, while projecting parameters
 333 to valid ranges to improve numerical stability.
- 334

336 Our setting is an unpaired text-to-appearance optimiza-
 337 tion problem: for each mesh we are given only a text in-
 338 struction and no reference image. As a result, pixel-based
 339 metrics (e.g., PSNR, SSIM) are not applicable. We also
 340 do not report other numerical metrics in this work, because
 341 they can be misleading for small-scale, open-ended appear-
 342 ance targets.

343 Instead, we adopt a tentative evaluation protocol based
 344 on a vision-language model (VLM) as a blind judge. For
 345 each trial, we render a single 2×3 comparison figure where
 346 the top row is *Ours* and the bottom row is *CLIP-only*. Each
 347 column corresponds to one object (Dolphin, Teapot, Tree),
 348 and the target prompt is shown under each column. We then
 349 ask the VLM to decide the overall winner across the three
 350 objects, focusing only on visible prompt adherence and ob-
 351 ject visibility.

352 We use the following evaluation prompt verbatim:

Unpaired	Text-to-Appearance	Evaluation	Instructions
Role: You are an evaluator for an unpaired text-to-appearance task.			
You will see ONE 2×3 comparison figure:			
<ul style="list-style-type: none"> • Top row = Ours • Bottom row = CLIP-only • Columns are three objects: Dolphin, Teapot, Tree. • Each column has its target prompt shown under the images. 			
Task: Decide which method is better overall across the 3 objects.			
How to judge (only what is visible):			
<ul style="list-style-type: none"> • Prompt adherence: color, material (glossy/matte), lighting, fog/no-fog, vignette, background • Object visibility: object should be clearly visible (not too dark or washed out) • Attribute correctness matters more than aesthetics 			
Output format (strict):			
WINNER = OURS or CLIP-ONLY or TIE			
REASON = one sentence summary			

4.2. Benchmark Comparison: Ours vs CLIP-only

Figure 2 shows the 2×3 comparison across Dolphin, Teapot, and Tree, with each target prompt displayed under its corresponding column. Using the evaluation protocol above, the VLM returned:

WINNER OURS

REASON Ours matches the key prompt attributes much better overall (teal glossy dolphin on a light studio background and a blue-fog vignetted tree silhouette), while CLIP-only is mostly too dark/off-color despite slightly better teapot visibility.

Qualitative analysis. For **Dolphin**, our output achieves a clearly visible teal subject against a bright studio-like background, whereas the CLIP-only baseline collapses to a dark, low-contrast rendering that obscures the object. For **Tree**, our method produces a recognizable silhouette and better conveys the requested cool fog and vignette, while the CLIP-only baseline again yields an under-exposed result with weak subject–background separation. For **Teapot**, the judge preferred the CLIP-only baseline mainly due to higher visibility. This indicates that visibility and exposure can be a failure mode in similarity-driven optimization, and that additional constraints may occasionally over-

377 restrict the search and lead to under-exposed outputs for
 378 dark materials.

379 4.3. Ablation: Concrete vs Abstract Instructions

380 Figure 3 compares two prompts that describe the same
 381 scene at different levels of specificity. The **concrete**
 382 prompt specifies directly controllable attributes (matte black,
 383 warm soft light, no fog), while the **abstract** prompt describes a
 384 high-level mood (quiet, cozy) without explicit appearance
 385 variables.

386 **Observation.** Although the abstract prompt is semanti-
 387 cally underspecified and does not explicitly name renderer-
 388 controllable attributes, our inverse rendering procedure still
 389 produces an output that remains contextually consistent
 390 with the concrete instruction. As shown in Fig. 3, both
 391 prompts lead to a similar overall “studio teapot” interpre-
 392 tation under a dark background, with the main discrepancy
 393 primarily reflected in secondary appearance choices such
 394 as highlight emphasis, rim-like responses, and the relative
 395 scale of the teapot. This suggests that our method can pre-
 396 serve scene-level context and produce semantically aligned
 397 renderings even when the text instruction is vague, while
 398 concrete prompts mainly act as stronger constraints that re-
 399 duce ambiguity in the final appearance.

400 4.4. Ablation: Prompt Length Extension

401 Figure 4 evaluates sensitivity to prompt length by progres-
 402 sively extending a base teapot instruction: (1) object and
 403 background description only, (2) plus explicit key light and
 404 rim light, (3) plus global tone controls (high contrast, slight
 405 vignette) and an explicit no fog constraint.

406 **Observation.** Fig. 4 shows that as we progressively ex-
 407 tend the prompt with additional, renderer-controllable con-
 408 straints, our method can reliably steer the same underly-
 409 ing scene toward more specific target conditions. Even
 410 the shortest instruction already yields a plausible solution
 411 (glowing green teapot on a magenta studio background),
 412 while the longer prompts refine the result in predictable
 413 directions by tightening lighting and post-processing re-
 414 quirements. In particular, adding explicit key and rim
 415 lighting encourages stronger, more structured specular re-
 416 sponses, and further appending high-contrast and vignette
 417 constraints produces a more stylized global tone without
 418 breaking object-background separation. Overall, this abla-
 419 tion highlights the controllability of our renderer: prompt
 420 augmentation provides extra constraints that reduce am-
 421 biguity, and the optimization can incorporate these addi-
 422 tional conditions to produce renderings that remain consis-
 423 tent with the intended appearance specification.

424 5. Conclusion

425 We presented a closed-loop approach for unpaired text-to-
 426 appearance inverse rendering that optimizes a differentiable

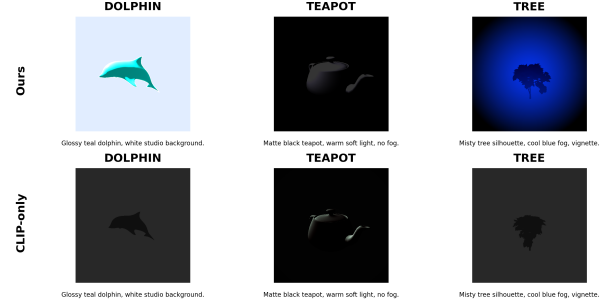


Figure 2. Benchmark comparison. Top row: *Ours*. Bottom row: *CLIP-only*. Columns correspond to Dolphin, Teapot, and Tree, with the target prompt shown under each column.

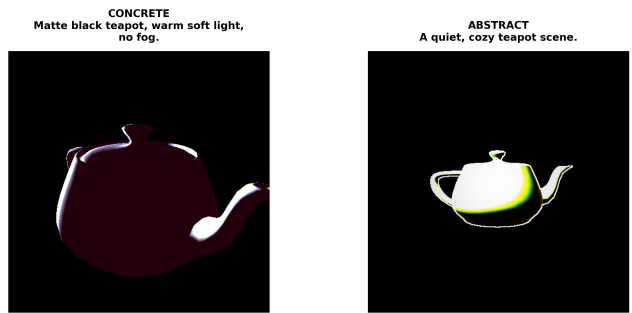


Figure 3. Concrete vs abstract prompt ablation on the teapot. The concrete prompt specifies renderer-controllable attributes, while the abstract prompt describes a high-level mood.



Figure 4. Prompt length extension ablation on the teapot. We progressively extend the prompt with explicit lighting and global tone constraints.

427 renderer’s controllable parameters using vision-language
 428 guidance. The key idea is to reduce ambiguity and insta-
 429 bility in CLIP-only optimization by introducing two forms
 430 of structured guidance: swap-safe prompt augmentation de-
 431 rived from foreground and background attribute parsing,
 432 and a parameter confiner that proposes an optimization plan
 433 with a top- K update set and tightened ranges. Across a
 434 benchmark comparison, our method achieves better overall
 435 prompt adherence than the naive CLIP baseline. In abla-
 436 tions, we find that the method produces contextually con-
 437 sistent results even when the text is abstract, indicating ro-
 438 bustness to underspecified semantics. Moreover, extend-

439 ing the prompt with additional constraints yields predictable
 440 changes in appearance, demonstrating that the renderer re-
 441 mains controllable and can incorporate augmented infor-
 442 mation without collapsing optimization. Our current eval-
 443 uation relies on pairwise visual judgments from a vision-
 444 language evaluator, which is suitable for an unpaired gen-
 445 erative setting but remains imperfect. Future work includes
 446 broader object and material coverage, stronger multi-view
 447 consistency constraints, and more systematic human stud-
 448 ies, as well as extending the framework to richer scenes and
 449 more physically grounded rendering models.

450 Author Contributions

- 451 • **Chi-Chang Lee** - co-proposed the LLM confiner module,
 452 co-developed the core pipeline that combines large lan-
 453 guage models with CLIP-based optimization, contributed
 454 advanced designs for integrating (visual) large language
 455 models with CLIP guidance as the confining strategy, and
 456 led the paper writing and overall presentation of the work.
- 457 • **Wenxuan Wu** - co-proposed the Vibe rendering frame-
 458 work, implemented the initial CLIP-only baseline, and
 459 co-developed the core pipeline that combines large lan-
 460 guage models with CLIP-based optimization.

461 References

- 462 [1] Tim Brooks, Aleksander Holynski, and Alexei A. Efros. In-
 463 structpix2pix: Learning to follow image editing instructions.
 464 In *Proceedings of the IEEE/CVF Conference on Computer
 465 Vision and Pattern Recognition (CVPR)*, 2023. 1, 2
- 466 [2] Ayaan Haque, Matthew Tancik, Alexei A. Efros, Alek-
 467 sander Holynski, and Angjoo Kanazawa. Instruct-nerf2nerf:
 468 Editing 3d scenes with instructions. *arXiv preprint
 469 arXiv:2303.12789*, 2023. 1, 2
- 470 [3] Nasir Mohammad Khalid, Tianhao Xie, Eugene Belilovsky,
 471 and Tiberiu Popa. Clip-mesh: Generating textured meshes
 472 from text using pretrained image-text models. In *SIGGRAPH
 473 Asia 2022 Conference Papers (SA '22)*. ACM, 2022. 1, 2
- 474 [4] Zhengqin Li, Mohammad Shafiei, Ravi Ramamoorthi,
 475 Kalyan Sunkavalli, and Manmohan Chandraker. Inverse ren-
 476 dering for complex indoor scenes: Shape, spatially-varying
 477 lighting and svbrdf from a single image. In *Proceedings of
 478 the IEEE/CVF Conference on Computer Vision and Pattern
 479 Recognition (CVPR)*, 2020. 1, 2
- 480 [5] Chen-Hsuan Lin, Jun Gao, Luming Tang, Towaki Takikawa,
 481 Xiaohui Zeng, Xun Huang, Karsten Kreis, Sanja Fi-
 482 dler, Ming-Yu Liu, and Tsung-Yi Lin. Magic3d: High-
 483 resolution text-to-3d content creation. *arXiv preprint
 484 arXiv:2211.10440*, 2022. 1, 2
- 485 [6] Gustavo Patow and Xavier Pueyo. A survey of inverse ren-
 486 dering problems. *Computer Graphics Forum*, 22(4):663–
 487 687, 2003. 1, 2
- 488 [7] Ben Poole, Ajay Jain, Jonathan T. Barron, and Ben Milden-
 489 hall. Dreamfusion: Text-to-3d using 2d diffusion. *arXiv
 490 preprint arXiv:2209.14988*, 2022. 1, 2

- 491 [8] Ravi Ramamoorthi and Pat Hanrahan. A signal-processing
 492 framework for inverse rendering. In *Proceedings of the 28th
 493 Annual Conference on Computer Graphics and Interactive
 494 Techniques (SIGGRAPH '01)*, pages 117–128. ACM, 2001.
 495 1, 2
- 496 [9] Soumyadip Sengupta, Jinwei Gu, Kihwan Kim, Guilin Liu,
 497 David W. Jacobs, and Jan Kautz. Neural inverse rendering
 498 of an indoor scene from a single image. In *Proceedings of
 499 the IEEE/CVF International Conference on Computer Vision
 500 (ICCV)*, 2019. 1, 2
- 501 [10] Zhengyi Wang, Cheng Lu, Yikai Wang, Fan Bao, Chongxuan
 502 Li, Hang Su, and Jun Zhu. Prolificdreamer: High-fidelity and
 503 diverse text-to-3d generation with variational score distilla-
 504 tion. *arXiv preprint arXiv:2305.16213*, 2023. 1, 2